Proceedings of ASME Turbo Expo 2011
GT2011
June 6-10, 2011, Vancouver, British Columbia, Canada

GT2011-46619

EVALUATION OF CFD PREDICTIONS USING THERMAL FIELD MEASUREMENTS ON A SIMULATED FILM COOLED TURBINE BLADE LEADING EDGE

SIBI MATHEW
The University of Texas at Austin
Austin, Texas, USA

SILVIA RAVELLI
University of Bergamo
Bergamo, ITALY

DAVID G. BOGARD
The University of Texas at Austin
Austin, Texas, USA

ABSTRACT

Computational Fluid Dynamics (CFD) predictions of film cooling performance for gas turbine airfoils are an important part of the design process for turbine cooling. Typically, industry relies on the approach based on Reynolds Averaged Navier Stokes equations, together with a two-equation turbulence model. The Realizable k-ε (RKE) model and the Shear Stress Transport k-ω (SST) model are recognized as the most reliable. Their accuracy is generally assessed by comparing to experimentally measured adiabatic effectiveness. In this study, the performances of the RKE and SST models were evaluated by comparing predicted and measured thermal fields in a turbine blade leading edge with three rows of cooling holes, positioned along the stagnation line and at ±25°. Predictions and measurements were done with high thermal conductivity models which simulated the conjugate heat transfer effects between the coolant flow and the solid. Particular attention was placed on the thermal fields along the stagnation line, and immediately downstream of the off-stagnation line row of holes. Conventional evaluations in terms of adiabatic effectiveness were also carried out. Predictions of coolant flows at the stagnation line were significantly different when using the two different turbulence models. For a blowing ratio of M = 2.0, the predictions with the SST model showed coolant jet separation at the stagnation line, while the RKE predictions showed no separation. Experimental measurements showed that there was coolant jet separation at the stagnation line, but the actual thermal fields obtained from experimental measurements were significantly different from that predicted by either turbulence model. Similar results were seen for predicted and measured thermal fields downstream of the off-stagnation row of holes.

INTRODUCTION

Modern gas turbines operate at temperatures higher than the melting temperature of the turbine blade and vanes materials. With advances in alloy and manufacturing technology, turbine operators have been able to increase gas turbine operating temperatures and consequently engine efficiency. Even then, cooling techniques are necessary for maintaining turbine blade integrity. Coolant air is usually impinged onto the interior surface to promote heat convection then it is ejected through holes formed in the airfoil walls to provide a flow of lower temperature coolant over the external surface of the airfoil. However, the airfoil is subject to a non-uniform external heat load distribution with the highest load being near the leading edge of the airfoil, due to the large heat transfer coefficient along the stagnation line. The common approach to the protection of this critical region is to incorporate a dense array of discrete film cooling holes, typically referred as the showerhead. Several experimental tests have been carried out to investigate the coolant dispersion into the mainstream over the leading edge. Thermal fields and flow visualization by Cutbirth and Bogard [1] showed that coolant jets in the showerhead region do not stay attached to the surface, even at relatively low blowing ratios. This can be explained by the lack of a crossflow along the stagnation line that would help in turning the coolant jets toward the surface and by the deceleration of the main flow as it comes close to the surface [2].

The comprehensive understanding of the main flow interaction with the coolant is even more important in light of the fact that the blade surface temperature is dominated by the effects of the external cooling. A combined experimental and modeling effort has been carried out in the recent years with the advent of larger computer resources. Several papers dealt with CFD predictions of film cooling with most studies utilizing codes based on the Reynolds Averaged

Navier Stokes (RANS) equations. Different turbulence models have been tested, such as Reynold's stress model (RSM), k-ε and k-ω. York and Leylek [3] indicated that adiabatic effectiveness, flow field and heat transfer coefficients were better predicted with the realizable model compared to the standard k-ε model (SKE) for film cooling applications on a leading edge. The deficiency of the SKE model was also brought to light by Medic and Durbin [4]: the predicted higher turbulence viscosity levels caused high temperatures to penetrate from the freestream closer to the blade surface. Harrison and Bogard [5] simulated film cooling on a flat plate model and compared results obtained using the RKE model, the standard k-ω (SKW) and RSM turbulence models. The SKW model showed the best comparison with the experimental data for laterally averaged adiabatic effectiveness values downstream of the exit hole at both $M = 0.5$ and $M = 1$. Even though the centerline adiabatic effectiveness was overestimated by all three turbulence models, the RKE model showed the best prediction at both blowing ratios while SKW and RSM indicated separation and reattachment of the coolant jet. Keimasi et al. [6] modeled jets in cross flow using the SKE model with wall functions and the SST model. While the mean velocity profiles for both turbulence models agreed with experimental data, the turbulent kinetic values were overpredicted by both models. The authors attributed anisotropy of the flowfield as a possible source of error since k-ε and k-ω turbulence models are isotropic in nature.

In the present work, the RKE and the SST model were chosen because of their extra-value in predicting complex flowfield. The RKE model differs from SKE model in the formulation for turbulent viscosity and in the transport equation for the dissipation rate ε. The term "realizable" refers to certain mathematical constraints which ensure positivity of normal stresses and Schwarz inequality for shear stresses. It has been proven that RKE model predicts separated flows and complex secondary flow features more accurately than SKE. The SST model blends the accurate formulation of the k-ω model in the near-wall region with the robustness of k-ε model in the far field. The refinements included in the SST model, in comparison with the standard one, include a new definition of the turbulent viscosity together with different modeling constants [7].

Many studies supported the idea that k-ε models, especially RKE, perform better than the k–ω models in predicting the surface temperature distribution and hence, film cooling effectiveness. Silieti et al. [8] carried out a computational investigation of film cooling effectiveness on a gas turbine endwall with one cylindrical cooling hole. Results from five different models (SKE, RNG k-ε, RKE, SKE and SST) were validated against experimental data in terms of centerline film cooling effectiveness downstream cooling-hole. At a blowing ratio of 2.0, all turbulence models captured jet lift-off. Among them, the RKE model was found to provide the best agreement with measurements whereas, the other four models under predicted film cooling effectiveness. In a following work [9], a parallel research on the same endwall was developed for one fan shaped cooling hole. The RKE and SST models as well as the v^2-f turbulence model were taken into account. Once again, the comparison with measured values of centerline cooling effectiveness downstream cooling-hole established the RKE model as the most reliable. In a comparative study, Na et al. [10] simulated film cooling by using three different turbulence models, such as RKE, SST and Spalart-Allmaras. They investigated a semi-cylindrical leading edge with three staggered rows of compound-angle holes. The RKE converged to the steady-state solution (but not the SST model) and predicted laterally averaged adiabatic effectiveness surprisingly well. Liu et al. [11] pushed their research a little further and presented a method to improve the accuracy of computed film cooling effectiveness on a flat plate with a one row of cylindrical holes. The whole flow domain was divided into a viscosity-affected region and a fully-turbulent region. In the former, an isotropic one-equation model was employed while in the latter the RKE was used. A specific Prandtl number was also assigned to each region. Results showed that changing Prandtl has great influence on the computation of effectiveness. Great improvement can be achieved with laterally varying Prandtl even in the frame of the traditional isotropic turbulence models.

Conversely, other surveys are in favor of the SST model. Lee and Kim [12] simulated and optimized film cooling through cylindrical and fan-shaped holes by means of the SST model. Spatially averaged film cooling effectiveness was maximized as a function of geometric variables, such as hole length to diameter ratio, ejection angle, and lateral expansion angle. An optimized hole shape was computed to increase film cooling effectiveness by 28% in comparison with the reference geometry. Simulations was performed with the SST model, which predictions of local and averaged film-cooling effectiveness agreed well with experimental data. The SST model was also chosen by Krishnababu et al. [14] to analyze flow field and heat transfer in a turbine rotor tip. Simulations were a needful tool to compare three different modifications, made to a standard blade tip, in an attempt to reduce the tip leakage mass flow. An assessment of different turbulence models was achieved by Ledezma et al. [15] for conjugate heat transfer in a turbine vane. The validation cases were an internally cooled vane and an internally and film cooled vane. Predictions obtained from different modeling strategies were compared to documented metal surface temperatures. In both cases, measurements of midspan temperatures showed good agreement with the SST predictions. However, predictions of heat transfer coefficient at midspan were less accurate downstream of the leading edge, on the pressure side.

In all the computational studies cited so far, validation of turbulence models was done against surface contours of adiabatic effectiveness or overall effectiveness. This kind of analysis gives an idea of the coolant footprint over a surface but does not provide information about coolant dispersion into the mainstream. Thermal field investigations are needed to overcome this limit. Lin and Shih [16] compared thermal field predictions from the SST turbulence model to experimental data by Cruse et al. [17]. They studied film cooling on a leading edge adiabatic model with stagnation and off stagnation rows of cooling holes. Thermal field data was measured by means of a thermocouple rake that included 10 type E thermocouple sensors, 0.1 mm in diameter. With the SST model, the normal spreading was under predicted from 20% to 50%. Even though the laterally averaged surface effectiveness was well simulated, the lateral spreading was over predicted above the surface, but under predicted on the surface. Moreover, the core of the computed coolant jet was significantly colder compared to measurements.

In a similar way, the aim of the current study was to validate CFD modeling of complex flow fields using thermal field measurements. Computations and experiments were run to investigate film cooling effectiveness and thermal field contours for a turbine blade leading edge with stagnation and off stagnation rows of cooling holes. The RKE and the SST turbulence models were chosen because of their superior performance in predicting film cooling results, when compared to other RANS turbulence models. High thermal conductivity models were used in experiments; meanwhile, the simulations included conjugate heat transfer in the solid. The comparison between thermal field measurements and numerical predictions was carried out along the stagnation line and in some downstream locations. The contribution of this paper to the body of literature consisted in employing off the wall measured temperatures to validate modeling. To the authors' knowledge, none of the previous studies documented a quantitative investigation of the thermal field on the stagnation line. Thakur et al. [18] modeled the same leading edge and predicted thermal fields but they only offered a qualitative evaluation of some typical off-the-wall aspects. Interaction between coolant and mainstream as well as jet-to-jet interaction were discussed without any support from experimental data. On the opposite, the current analysis was based on measurements and aimed at providing not only a better understanding of the coolant interaction with the mainstream all over the leading edge surface but also an idea of turbulence models potential and limitations.

NOMENCLATURE

Symbols

Bi	Biot number = *ht/k*
d	Diameter of cooling holes
DR	Density ratio DR = ρ_c / ρ_∞
h	Convective heat transfer coefficient
k	Thermal conductivity
K	Turbulent kinetic energy
l	Turbulent length scale
M	Blowing ratio = $\rho_c U_c / \rho_\infty U_\infty$
p	Hole-to-hole pitch
RKE	Realizable k-ε
SST	Shear stress transport k-ω
t	Airfoil wall thickness
Tu	Turbulence intensity
x, y, z	Reference coordinates
y^+	Non dimensional distance from the wall
T	Temperature
η	Adiabatic effectiveness $\eta = (T_{aw} - T_\infty)/(T_c - T_\infty)$
ϕ	Overall effectiveness $\phi = (T_w - T_\infty)/(T_c - T_\infty)$
θ	Normalized temperature $\theta = (T_{gas} - T_\infty)/(T_{c,out} - T_\infty)$

Subscripts and Superscripts

aw	Adiabatic wall
c	Coolant
out	Exit
sh	Showerhead
w	Wall
∞	Approach flow
‗	Lateral average

EXPERIMENTAL SETUP AND PROCEDURE

All experiments for this study were conducted in the closed loop wind tunnel facility (Figure 1) which had already been used in numerous previous works by Albert et al. [19], Terrell et al. [20] and Dyson et al. [21]. Hot mainstream gas was simulated by room temperature air, driven by a 5 hp axial fan. An average mainstream temperature of 300 K was maintained during the experiments by means of a heat exchanger. Cylindrical vertical bars were located at the beginning of the test section in order to generate a high level of turbulence in the flow. The leading edge model was placed within the test section at a distance of 0.38 m from the turbulence generators. The turbulence intensity and the integral length scale were measured to be *Tu* = 6% and *l* = 20 mm (6*d*), respectively. The 9:1 area contraction in the wind tunnel geometry resulted in a 0.61 m wide and 0.15 m high test section. During experiments, the mainstream air had a constant velocity of 15 m/s resulting in Reynolds number of 48,000, based on leading edge diameter. The coolant used in the film cooling process was cold nitrogen gas, maintained at a temperature of 200 K during the experiments in order to achieve a density ratio *DR* = 1.5. Since nitrogen was available in liquid form at a temperature of 77 K, a preheating system was necessary to vaporize the nitrogen and to warm it to the desired temperature. Nitrogen flowed first through electrical resistance heating elements then passed through a heat exchanger where the mainstream tunnel air was rerouted. The coolant then entered an insulated plenum attached to the leading edge model. Dehumidification of the mainstream air was also performed to avoid frost accumulation; the relative humidity in the air was reduced to about 4% before data was collected for the experiments.

Film cooling performance was evaluated on a scaled up model of a typical turbine blade leading edge. Two models with the same geometry were constructed: the almost adiabatic model (*k* = 0.03 W/mK) and the conducting model (*k* = 1.04 W/mK). The first model was necessary to determine adiabatic effectiveness η values whereas the second one was used to measure off the wall thermal profiles. The Biot number for the conducting model was matched to that for operational engine conditions. As shown in Figure 2, the model consisted of a cylindrical leading edge section and a flat section extending behind it. The external and the internal diameter of the leading edge were 50.8 mm and 25.4 mm, respectively.

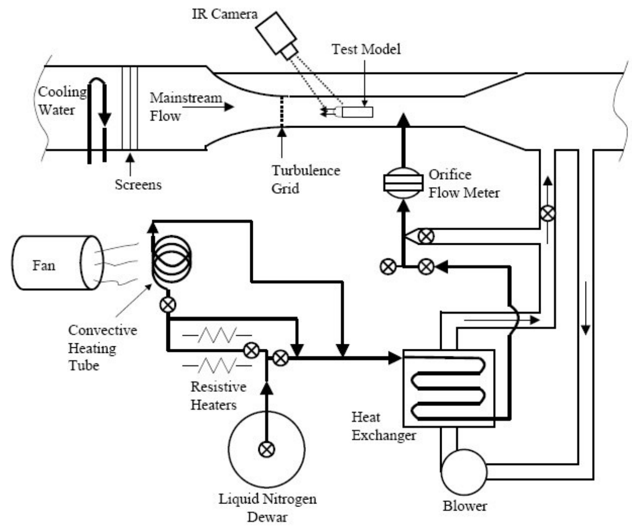

Figure 1: Schematic of the wind tunnel facility

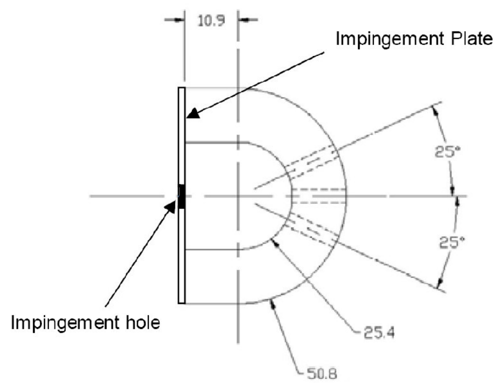

Figure 2: Side view of the leading edge model

The film cooling configuration included three rows of holes positioned along the stagnation line and at ±25° from the stagnation line. The diameter of each hole was *d* = 3.18 mm. The holes were angled at 20° to the surface and oriented normally to the flow direction (i.e. 90° compound angle). Within each row, the hole-to-hole pitch was *p* = 24.2 mm, resulting in a *p/d* = 7.6. The impingement plate had holes 5 mm in diameter and directed the coolant from the plenum towards the internal surface of the model in the form of high velocity jets.

The coolant volumetric flow rate was measured using an orifice meter that was located upstream of the plenum reservoir. The mainstream velocity was measured by means of a Pitot static probe. All temperature measurements in the wind tunnel were obtained from E-type thermocouples. The mainstream thermocouple was located well upstream of the leading edge model. The coolant temperature was measured close to the orifice meter and within the plenum. This latter value was used to compute coolant density. All data coming from temperature and pressure transducers were input to a National Instrument DAQ system. Steady-state experiments were performed at constant *DR* = 1.5. The nominal blowing ratio was *M* = 2.0, with local blowing ratio of *M* = 1.95 and 2.03 at stagnation and off-stagnation rows, respectively. The blowing ratios for the stagnation and off-stagnation rows differed because of the variation of the external static pressure.

An E-Type thermocouple was used to collect off the wall temperature profiles. To minimize conduction errors, the thermocouple probe was constructed using 2-mil wires. Terrell et al. [20] carried out experiments with similar conditions (M = 2 and DR = 1.5) and they established that the conduction error with a 2-mil probe was negligible. Subsequently, the thermocouple probe was reinforced with a copper tube and mounted onto a traverse system (Figure 3) that was located within the test section of the wind tunnel. The main body of the traverse system consisted of two stepper motors, a pivoting system, a linear stage and rods spanning the test section. The thermocouple setup was chosen to minimize the impact of the probe arm on the interaction of the mainstream with the stagnation line coolant holes.

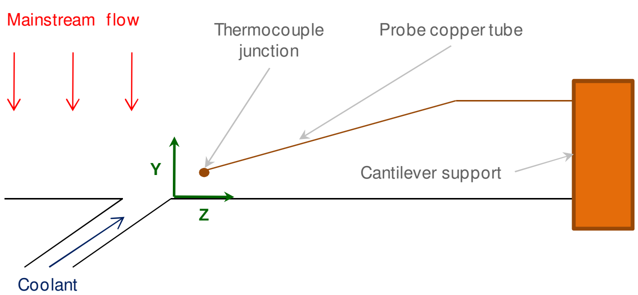

Figure 3: Schematic of the thermocouple probe with the traverse system

The accuracy of the measurements was verified by checking test-to-test repeatability. Figure 4 shows results from thermal profile measurements in terms of normalized gas temperature, i.e.

$$\theta = \frac{(T_{gas} - T_{\infty})}{(T_{c,out} - T_{\infty})} \qquad (1)$$

where $T_{c,out}$ is the coolant temperature at exit hole. The origin of the coordinate system was placed at the lip of the stagnation row exit hole. Axes were oriented as shown in Figure 5: x/d is downstream distance with respect to the symmetry plane; y/d indicates distance normal to the leading edge surface; finally, z/d represents distance in the spanwise direction. Off-the-wall thermal profiles were measured in separate experiments, *#1* and *#2*, for each position. At the stagnation plane (x/d = 0), test to test repeatability was checked at z/d = 2.5 and z/d = 7. Measurements of θ were generally repeatable within ± 0.02, except for the outer part of the thermal profile at x/d = 0 and z/d = 2.5 where it appears the height of the jet varied by about y/d = 0.2 between the two experiments. This slight difference in the coolant jet height may have been due to slightly different blowing ratios between the two experiments. Repeatability in measurements was also verified at a position just downstream of the off-stagnation row of holes at x/d = 5.1 and spanwise positions of z/d = 4.9 and z/d = 2.9. These locations were where the coldest footprint of the coolant and significant coolant separation occurred, respectively. In both cases, θ profiles revealed that experiments had good repeatability.

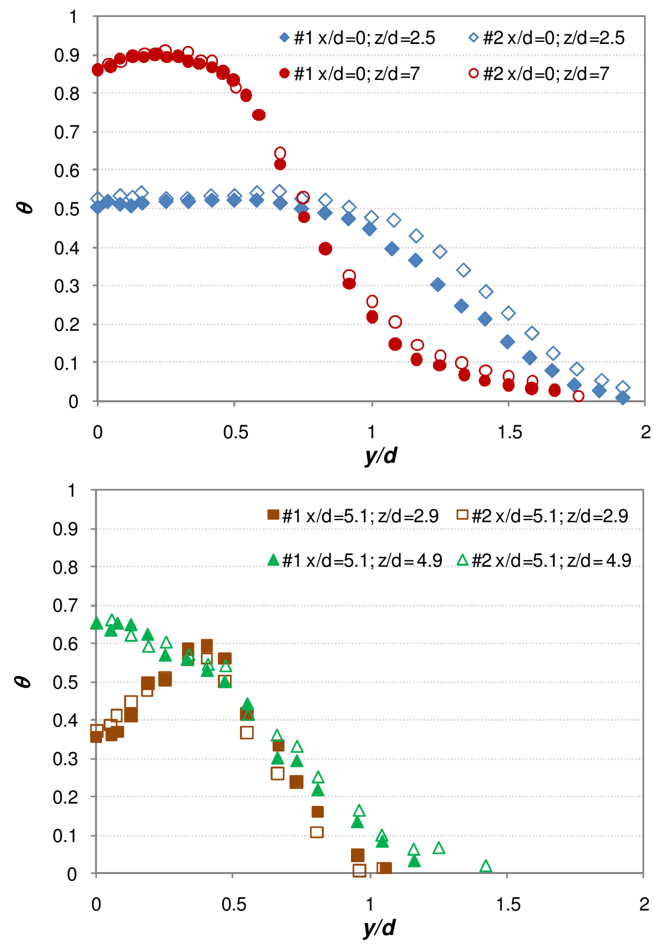

Figure 4. Repeatability tests for normalized temperature measurements

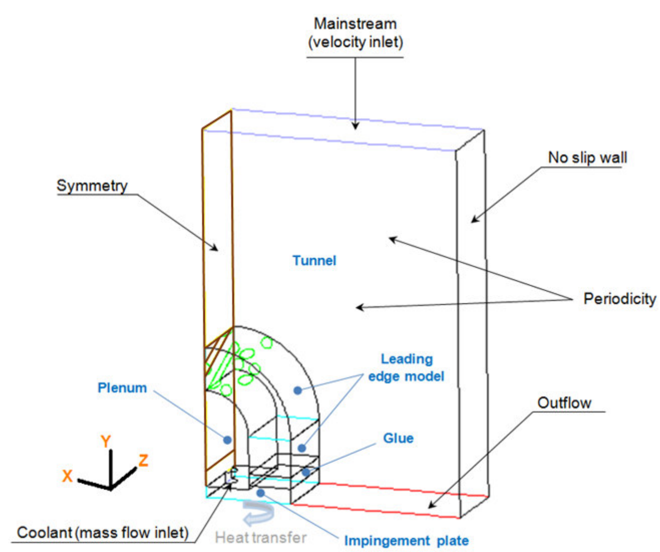

Figure 5. Schematic of the 3D computational domain

COMPUTATIONAL SETUP

The leading edge used in the computational study had the same geometry as the experimental model. A schematic of the 3D computational domain is shown in Figure 5. Only one pitch distance was computed in the simulations thanks to periodic planes. A symmetry condition was used at the stagnation plane thus enabling simulation of only half the model. The boundary conditions listed in Table 1 matched the experiments. The mainstream inlet was characterized in terms of temperature, constant velocity, turbulence intensity and length scale. The injection of the coolant through the impingement hole was specified by a mass flow inlet condition: a value of 0.000411 kg/s was set to obtain a blowing ratio of $M = 2$ (averaged for all rows of holes). The coolant inlet turbulence intensity was set at an estimated value of $Tu = 6\%$ with a turbulence length scale of $l = 9.5$ mm. Air was used to model both the coolant and the mainstream. Air properties were set to be temperature dependent, according to polynomial relationships obtained from Mills [22]. A separate analysis of the impingement plate yielded the heat transfer coefficient of $h = 31.8$ W/m^{2}K used as the boundary condition on the external surface of the impingement plate. More details about the computational domain and the boundary conditions can be found in a previous paper by Ravelli et al. [23].

Conduction through the solid was simulated by setting a leading edge thermal conductivity of $k = 1.04$ M/mK, equal to the experimental model. All the solid-to-solid or solid-to-fluid interfaces were modeled according to the coupled thermal condition. On the other hand, the adiabatic simulation was done by deactivating the solid.

The CFD analysis was carried out by means of FLUENT version 6.3. The solution was designed to solve the steady flow by using implicit method. The pressure-based segregated solver was chosen together with a SIMPLE pressure-velocity coupling. In order to validate the ability of numerical modeling to adequately reproduce complex phenomena, two different turbulence models were considered: the RKE and the SST models. The transitional feature was not enabled because the flow is presumed to remain turbulent due to interaction of the mainstream with the coolant. The enhanced wall treatment function was activated along with thermal and pressure gradient effects. The intention of resolving the viscous sublayer required high grid resolution in the wall-adjacent region. A prism layer was thus attached to the leading edge external surface to capture coolant separation and jet spreading. The GAMBIT software was used to construct two unstructured tetrahedral grids, whose details along the symmetry plane are shown in Figure 6. The coarse mesh (Figure 6a) had a total of 5.4 millions cells whereas the fine mesh (Figure 6b) consisted of about 10 millions cells. Note also the differences in grid clustering at the exit of the cooling holes and in the prism layer thickness. Both the grids assured $y^+ < 4$. Grid independence was tested for each turbulence model: the coarse grid was found to provide grid independent solutions for the RKE turbulence model, while the SST model needed to be run with the fine mesh. The residuals were kept below 10^{-9} for energy and below 10^{-4} for the specific dissipation rate ω. All other residuals were kept below 10^{-6}. At convergence, the surface temperature at a point of high temperature gradient changed by no more than 0.01% for at least 200 iterations.

Table 1. Boundary conditions for the CFD model

Inlet mainstream velocity	m/s	15
Inlet mainstream temperature	K	300
Inlet mainstream turbulence intensity	%	5.9
Inlet mainstream turbulent length scale	mm	19
Coolant temperature	K	200
Coolant mass flow rate	kg/s	4.1e-4
Coolant turbulence intensity	%	6
Coolant turbulent length scale	mm	9.5

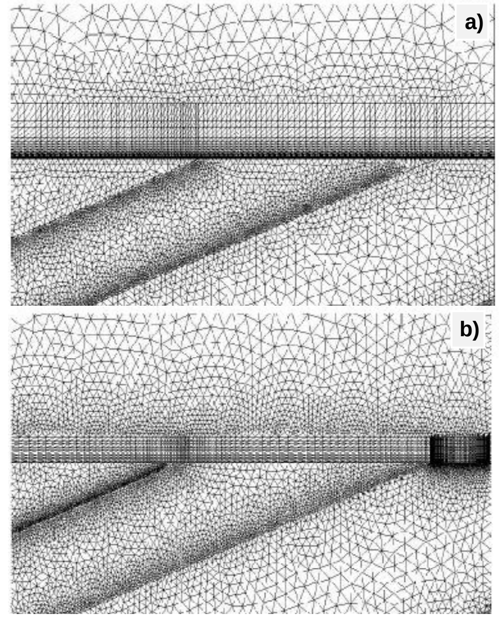

Figure 6. Grid resolution at the symmetry plane for the: a) coarse mesh, b) fine mesh

RESULTS AND DISCUSSION

CFD simulations of a film cooled model of a turbine blade leading edge with three rows of coolant holes were completed using the RKE and SST turbulence models. To evaluate these simulations, adiabatic effectiveness was measured around the leading edge model. However, the major focus of this study was the evaluation of the CFD predictions using measurements of the thermal fields collected above the surface which showed directly the separation of coolant jets and the dispersion of the coolant. These measurements were done at two critical positions: the plane normal to the stagnation line at the leading edge of the model, and a plane 1d downstream of the off-stagnation row of coolant holes. These results and evaluations are presented below.

Evaluation in terms of adiabatic effectiveness

Often the performance of CFD simulation has been evaluated by comparing the predicted laterally averaged adiabatic effectiveness with experimental measurements. This comparison for the leading edge geometry investigated in this study is presented in Figure 7. The predictions with the RKE model were in very good agreement with experimental measurements, while predictions with the SST model were generally 25% high. Based on this result one would conclude that accurate CFD simulations of film cooling could be achieved using the RKE turbulence models, but more detailed analysis shows that this is not the case.

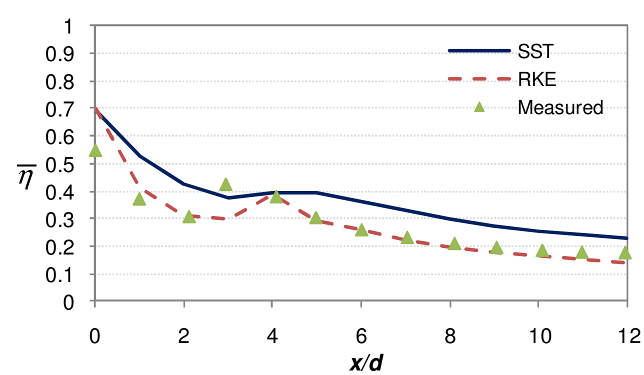

Figure 7. Predicted vs. measured laterally averaged adiabatic effectiveness

Comparisons of surface distributions of η for the CFD simulations and experimental measurements are presented in Figure 8 for M = 2 and DR = 1.5. These results show that there are significant differences between the SST and RKE turbulence models, and between the CFD simulations and the experiment. Focusing on the stagnation line (Figure 9), the RKE model predicted the highest η values close to the exit of the hole (z/d = 0) while the SST model predicted lower η closer to the hole exit with highest η values occurring closer to the leeward edge of the adjacent hole (z/d = 4.7). These results suggest that the SST model predicted coolant jet separation while the RKE model did not. As will be discussed later, this was confirmed by reviewing the thermal fields above the surface. Both CFD simulations predicted significantly higher η values along the stagnation line than measured experimentally. This prompted an interest in measuring the overflowing thermal field and comparing it to the predicted thermal fields. These results will be discussed later.

Also evident from the contour plots of η presented in Figure 8 is a difference in the path of coolant flow from the stagnation row of holes as it flows downstream. Arrows have been sketched on these plots showing the path of the coolant flow (based on peak effectiveness values). For the RKE simulation the coolant from the stagnation row of holes intersects the right edge of the downstream off-stagnation coolant holes. However, for the SST model the coolant travels farther in the spanwise direction before turning downstream. Consequently for the SST simulation the coolant flow fills in the gap between downstream off-stagnation coolant holes. The contour plots for the experimental measurements are more dispersed so the path of coolant flow is not as distinct, but the coolant flow path is more similar to that of the SST model, i.e. filling in the gap between off-stagnation holes.

Downstream of the off-stagnation coolant holes, the path of the coolant flow from off-stagnation holes is clear and the same in all cases. However, the η distributions were very different for the CFD simulations and the experimental measurements. Both SST and RKE models predicted η levels in the center of the coolant jet (indicated by peak effectiveness values) that were much higher than measured experimentally. Furthermore, the predicted distribution of coolant using the SST model was noticeably wider than predicted with the RKE model. A direct comparison of the η levels and distribution widths is presented in Figure 10 which shows the lateral distributions of η at x/d = 5.1, i.e. just 1d downstream of the coolant hole.

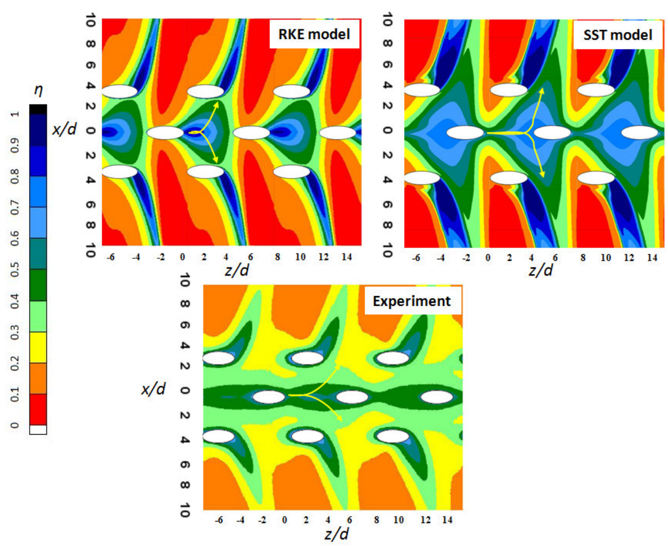

Figure 8. Predicted surface contours of adiabatic effectiveness according to RKE and SST models compared with experimental data

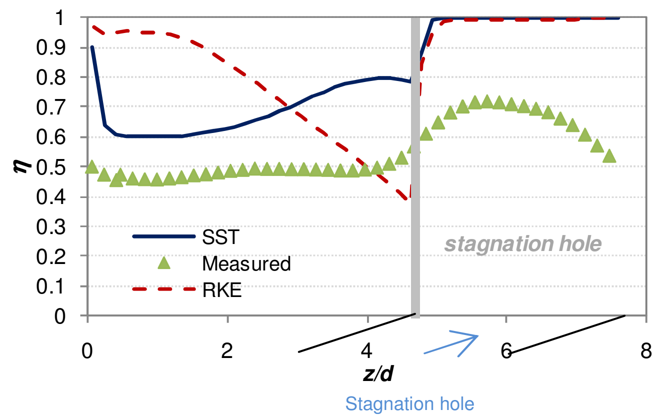

Figure 9. Predicted vs. measured adiabatic effectiveness at stagnation line (x/d = 0)

From Figure 10 it is evident that both CFD simulations predict much higher peak levels of $\eta > 0.9$ while the experimental measured peak level was η = 0.5. The lower level of η measured suggest that the actual coolant jet separated from the surface while the CFD simulations did not predict separation. This was examined in more detail with thermal field predictions and measurements at x/d = 5.1 which will be discussed later.

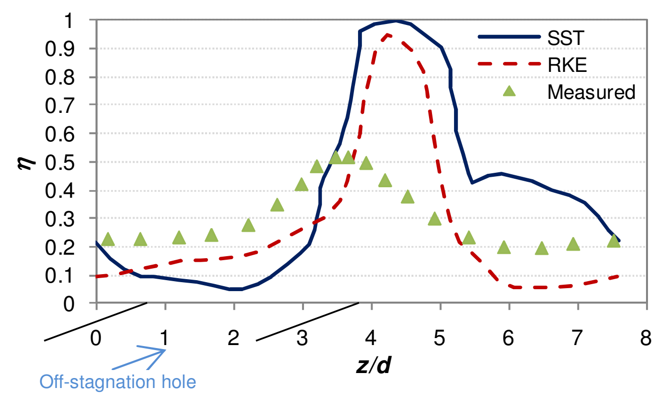

Figure 10. Predicted vs. measured adiabatic effectiveness at x/d = 5.1

Flow field analysis in the stagnation plane

CFD simulations and experimental measurements of thermal fields above the wall were done using a high conductivity leading edge model whose Biot number matched typical engine conditions. This was done in order to include conjugate heat transfer effects. However, thermal profiles for adiabatic and conducting models were found to be very similar, with only a small difference when approaching the wall. Figure 11 shows the predicted profiles of normalized temperature θ along the stagnation plane, at z/d = 2.5, according to the SST turbulence model. Clearly the temperature profiles over the conducting wall were essentially the same at those over an adiabatic wall. As expected, profiles differed only close to the wall, specifically $y/d < 0.1$.

Direct evaluation of the dispersion of the coolant jet from the stagnation line row of holes was obtained by comparing predicted and measured thermal fields in a plane normal to the wall at the stagnation line as shown in Figure 12. The contour plots of normalized temperature θ presented in Figure 12 clearly show the coolant with $\theta > 0.9$ at the exit of the coolant hole for CFD simulations and the experimental measurements. There were two significant differences between the predictions using the SST model and the RKE model. First the SST model showed a clear separation of the coolant jet while the RKE model did not. Second, the dispersion of the coolant (indicated by the decrease in θ values) was greater for the RKE model than for the SST model. Comparison to the experimental measurements showed that neither the SST model nor the RKE model provided a good simulation of the actual jet profile along the stagnation line. The experimental measurements did confirm that there was jet separation as predicted by the SST model, but the dispersion of the coolant jet was much greater than predicted by the SST model, all though less than predicted by the RKE model.

A better comprehension of the discrepancies in coolant dispersion between modeling and experiments is obtained by direct comparison of temperature profiles at different span locations along the stagnation plane as shown in Figure 13. At a position at the edge of the hole, z/d = 0, the simulated and measured coolant jet thermal profiles were of similar, each showing a peak of θ = 0.9. Note that the coolant temperature at the exit of the hole increased from the internal coolant temperature of θ = 1.0 because the coolant is heated as it flows through the hole. The fact that the peak θ value at the exit of the hole was similar for both simulations and the experiment is important because it shows that convective warming of the coolant was modeled well by the CFD simulations using both the SST and RKE turbulence models. Slightly farther from the hole exit, and z/d = 2, the temperature profiles for the simulations and the experiment were very different. The SST model simulation showed a distinct peak in θ above the wall indicative of coolant jet separation.

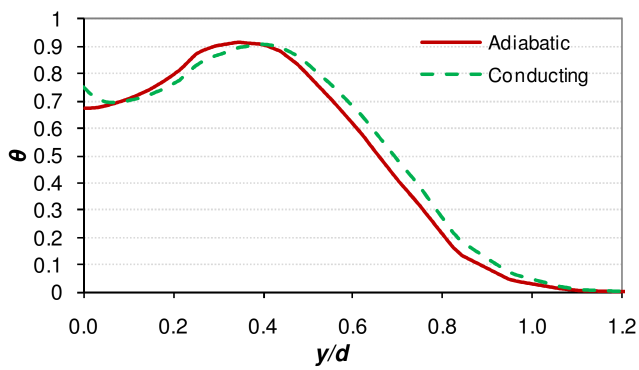

Figure 11. Adiabatic vs. conducting normalized temperature profile at *x/d* = 0 and *z/d* = 2.5

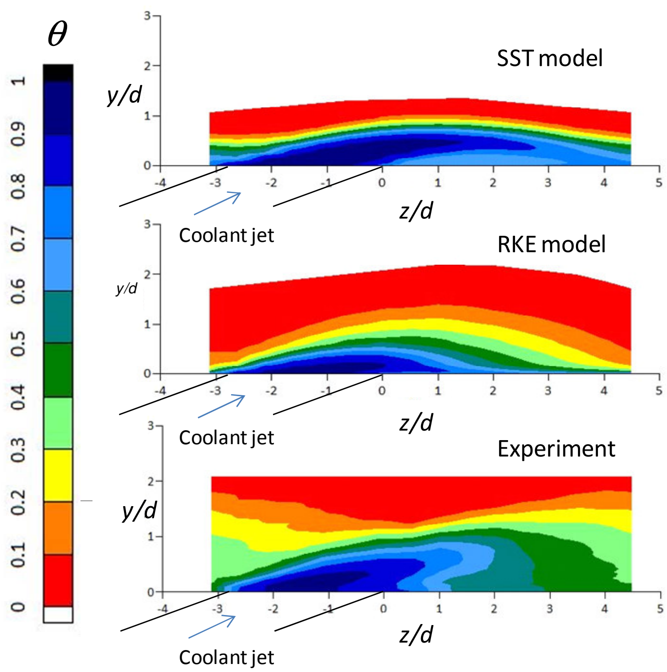

Figure 12. Predicted normalized temperature contours along stagnation plane, according to SST model, RKE model compared with experimental data

Measurements also showed a peak in θ above the wall, but substantially smaller in magnitude than the SST model simulation, indicating the actual dispersion of the coolant jet was much larger than predicted by the SST simulation. The RKE simulation did not show any peak in θ, i.e. no separation, and generally had much lower levels of θ suggesting prediction of higher levels of coolant dispersion than measured. Similarly, at z/d = 4, the predicted temperature profiles using CFD simulations with the RKE and SST models were very different, and each of these simulations were very different from the actual profile measured experimentally. The measured peak level of θ = 0.4 was much less than the predicted peak values of θ = 0.7 to 0.75. Experimentally significant coolant levels (θ > 0.1) were measured to extend to y/d = 1.8, but the CFD simulations with both turbulence models showed this coolant level extending only to y/d = 0.7.

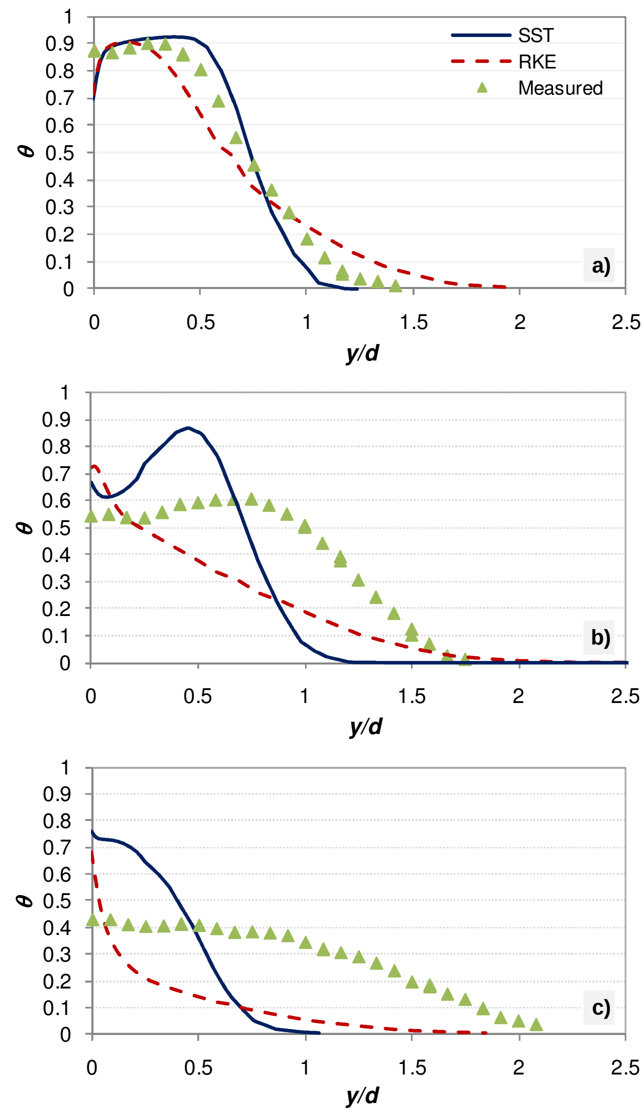

Figure 13. Predicted vs. measured normalized temperature profile along stagnation plane at a) *z/d* = 0 , b) *z/d* = 2, c) *z/d* = 4

To obtain more insight into why the SST turbulence model predicted coolant jet separation, but the RKE model did not, the predicted velocity fields at the exit of the coolant holes, shown in Figure 14, were compared. The distributions of velocity vectors shown in Figure 14 do not indicate any significant difference in the predicted velocity distribution at the exit of the hole. After the coolant jet exited the hole, the SST simulation showed a distinct separation bubble underneath the coolant jet flow, while the RKE model did not show any indication of separation. Figure 14 also provides confirmation that the the coolant flow at the inlet of the hole were similar for both turbulence models. In both cases the internal impingement jets looked very similar, and the separation region at the inlet of the hole were the same.

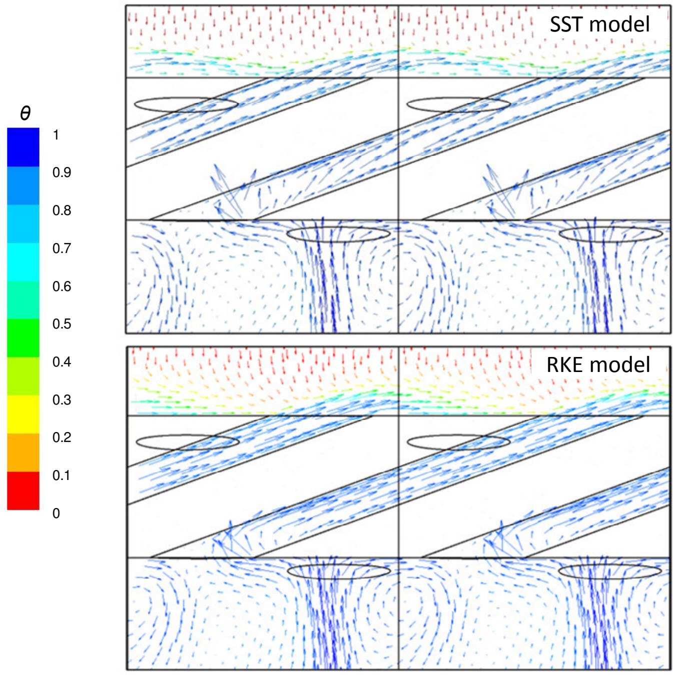

Figure 14. Predicted velocity vectors colored by normalized temperature along stagnation plane, according to SST model and RKE model

The turbulence levels predicted by the SST and RKE turbulence models were also examined to gain a better understanding of why the RKE model predicted greater dispersion of the coolant jets. The turbulence level, Tu, was defined as follows:

$$Tu = \frac{\sqrt{2k/3}}{U_\infty} \tag{2}$$

where k is the turbulent kinetic energy. Contours of simulated Tu levels along the stagnation plane for the RKE and SST turbulence models are presented in Figure 15. There was a very clear difference in the computed turbulence levels, with the prediction using the RKE model showing a broad range of increase turbulence level with peak levels in excess of Tu = 32%, while the SST model prediction was a very thin layer of higher turbulence levels located at the outer edge of the coolant jet. When comparing to the θ contours of Figure 12, the larger region of high turbulence for the RKE model was found to corresponded to the larger shear layer. However, it is not clear whether the predicted broader high turbulence region caused a broader shear layer, or vice versa. No measurements were made of the turbulence levels for the leading edge configuration tested, but previous measurements by Polanka et al. [24] on a simulated turbine vane leading edge showed very high turbulence levels with Tu > 30% in extending beyond y/d = 2 in the stagnation line region. So the RKE model predictions appeared to be the closest to measured values. Moreover experiments [24] revealed that turbulence is highly anisotropic, with the spanwise component of the turbulent fluctuations being twice as large as the other components. This cannot be simulated by RANS methods which assume isotropy of turbulence whereby the normal stresses are equal.

Flow field analysis downstream of stagnation line

As noted previously, the RKE and SST turbulence models predicted different coolant flow paths from the stagnation row of coolant holes. Although measurements were not made between the rows of cooling holes, comparisons of the SST and RKE predictions were carried out at this location to better determine differences between the two turbulence models.

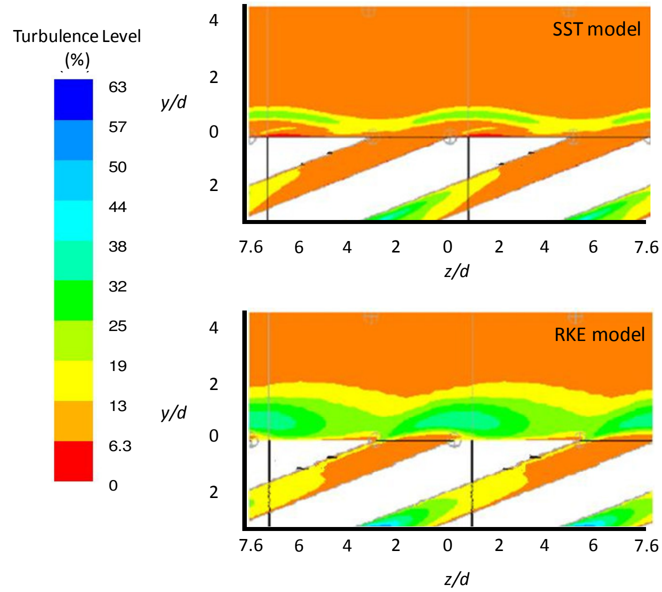

Figure 15. Predicted turbulence intensity contours along stagnation plane, according to SST model and RKE model

The predicted θ contours at x/d = 2 are shown in Figure 16. As expected, based on the previously presented adiabatic effectiveness contours, the SST model predicted a colder core of coolant flow than the RKE model. The position of the jet core was also different for the two models. In the SST case, the jet core was located further away from the stagnation hole lip, at about z/d = 4.2, compared to the core of the RKE coolant jet located at z/d = 2. This difference can be attributed to the SST model predicting jet separation which caused the jet to move a significant lateral distance before turning downstream. Furthermore the temperature gradients predicted by the RKE model were much broader than predicted by the SST model, indicating that the RKE model predicted larger dispersion of the coolant.

A second direct comparison of measured and predicted thermal fields above the wall was done at the x/d = 5.1 position, which was about 1d downstream of the off-stagnation row of holes. These thermal profiles are presented in Figure 17. The core of the coolant jet emanating from a coolant hole in the off-stagnation row of holes is clearly evident in these contour plots. CFD simulations and experimental measurements both show the coolant jet core twisted towards the negative z direction due to the impact of the mainstream on the jet emanating in the positive z direction. The general shape and magnitudes of the contours were very similar for the SST and RKE turbulence models. Compared to the experimental measurements, the CFD simulations predicted the coolant to extend about 30% farther from the surface. The CFD simulations also did not show the coolant flow distributed across the full pitch, whereas the experimental measurements showed contour levels above θ = 0.1. The higher θ values measured beyond the core of the coolant jet were due to coolant flowing from the stagnation row of holes. Reviewing the adiabatic effective contours in Figure 8, it appears that the CFD simulation did not predict higher levels across the full span at x/d = 5.1 because neither the SST model nor the RKE model predicted as much lateral spreading of the coolant from the stagnation line row of holes as was measured experimentally.

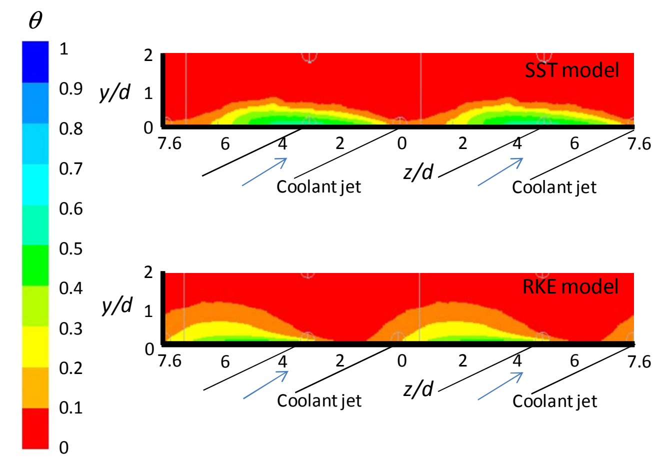

Figure 16. Predicted normalized temperature contours along *x/d* = 2 plane according to a) SST model b) RKE model

The accuracy of the simulations at *x/d* = 5.1 plane was also evaluated by comparing thermal profile from CFD simulations and experiments at two different *z/d* locations, as shown in Figure 18. The first location, z/d = 2.9, was a position where there was coolant separation from the surface while the second location, z/d = 4.9, where the experiments showed maximum θ at the surface. At *z/d* = 2.9, simulations with both RKE and SST models predicted the location of the peak θ values very similar to the experimental measurements, and the magnitudes of the near wall θ values and peak θ values were similar to the measured values. However the CFD simulations predicted noticeable coolant levels extending about 30% farther from the wall than was measured. At *z/d* = 4.9, the peak value of θ = 0.63 close to the surface is well predicted by the RKE while the SST simulation shows a slightly higher θ. The distance to the outer edge of coolant was also predicted well by both the RKE and SST models, but the measurements showed significantly higher θ values over the range $0.3 < y/d < 0.8$. This might be due to coolant flow from the stagnation row of holes that was not well predicted by the CFD simulations.

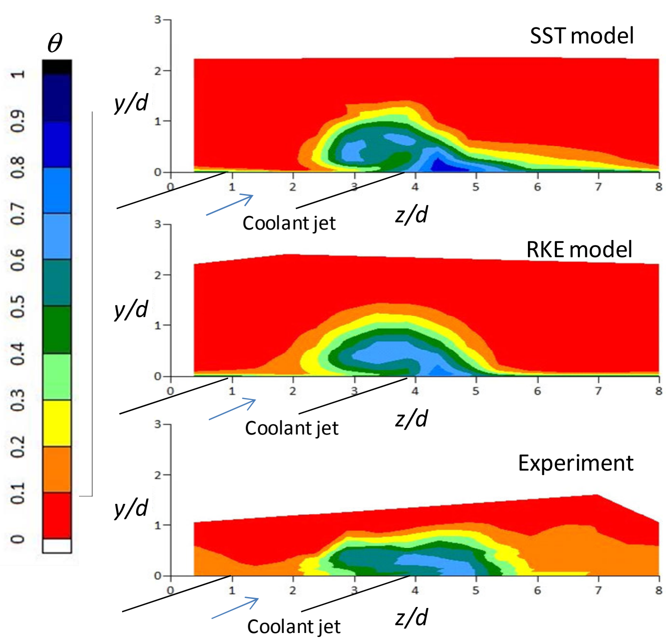

Figure 17. Predicted normalized temperature contours along *x/d* = 5.1 plane according to SST model, RKE model compared with experimental data

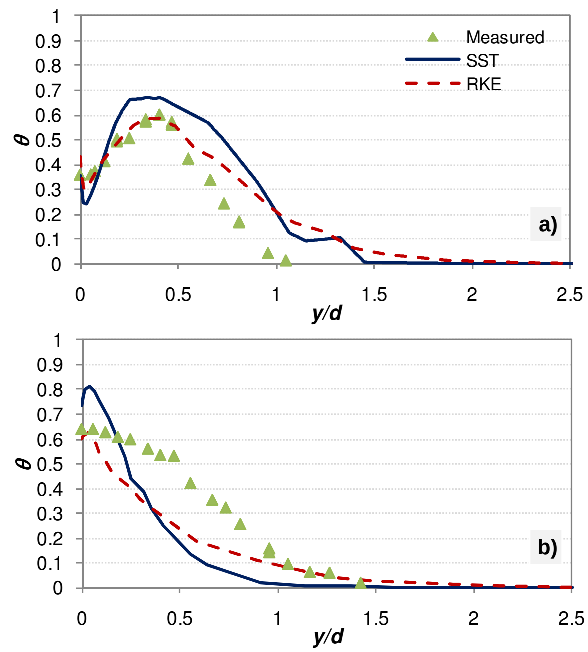

Figure 18. Predicted vs. measured normalized temperature profile along *x/d* = 5.1 plane at a) *z/d* = 2.9 , b) *z/d* = 4.9

Overall, the CFD simulations using both turbulence models provided much better predictions of the coolant jet emanating from the off-stagnation row of holes that from the stagnation row of holes. This may be due to the complexity of the flow in the stagnation plane relative to the cross-flow past the off-stagnation row of holes.

CONCLUSIONS

The focus of this study was to evaluate CFD predictions of film cooling on a leading edge model by comparing it to experimental results. The leading edge model had three rows of film cooling holes, with one row on the stagnation line and two additional off stagnation rows at ± 25°. The thermal conductivity of the conducting model was specified such that the Biot number of the model matched that for a typical engine blade. The RKE and SST turbulence models were selected for these simulations. All the analyses presented in this work were performed for a blowing ratio of M = 2 and a density ratio of DR = 1.5.

Conventional evaluations of the CFD simulations were done using measurements of adiabatic effectiveness. The RKE predictions of laterally averaged adiabatic effectiveness were in very good agreement with the experimental measurements whereas SST predictions were distinctly higher throughout the length of the leading edge. However, from surface contours adiabatic effectiveness, it was clear that neither the RKE nor SST turbulence models accurately predicted the adiabatic effectiveness distribution. This made clear that analysis based on laterally averaged values can lead to misleading conclusions. The downstream spreading of the coolant also differed between turbulence models. Experimental data revealed that coolant exiting from the stagnation holes joins the off stagnation row at a similar spanwise distance to the SST prediction.

Analyses of thermal profiles along the stagnation plane showed very different predictions using the RKE and SST models. The SST model predicted a distinct jet separation but no separation was predicted by the RKE model. Thermal field measurements in this plane showed that the coolant jets from the stagnation row of holes did separate as predicted by the SST model, but had a much greater dispersion of coolant than predicted by the SST model. The SST model was found to underpredict the turbulence generated by the coolant jet interaction with the approach flow, which is likely why the coolant dispersion was underpredicted. On the other hand, the RKE model overestimated the mixing process predicting greater dispersion of the coolant than observed experimentally.

An evaluation of the accuracy of the CFD was also done at a position immediately downstream of the off-stagnation row of holes. The general shape of the coolant emanating from the off-stagnation holes was properly predicted by both turbulence models, with the jet skewed to the left, in the direction opposite to coolant exit path. The location of the peak normalized temperature and magnitude were similar for simulations with both turbulence models and the experimental measurements. However, adiabatic effectiveness measurements showed that the CFD simulations predicted much higher peak adiabatic effectiveness levels than actually occurred.

In conclusion, neither the RKE nor SST turbulence models were found to adequately simulate the film cooling flow around a leading edge, particularly at the stagnation line. This may be an inherent limitation of RANS simulations, and accurate predictions of film cooling performance on a turbine airfoil leading edge may require more sophisticated CFD simulations such as an Unsteady-RANS or time resolved LES simulations.

ACKNOWLEDGEMENTS

The authors would like to thank to Office of Naval Research for funding this research through the ESRDC (Electric Ship Research and Development Consortium).

REFERENCES

[1] Cutbirth, J. M. and Bogard, D. G., 2001, “Thermal field and flow visualization within the stagnation region of a film cooled turbine vane”, ASME paper 2001-GT-0401.

[2] Bogard, D. G. and Thole, K. A., 2006, “Gas Turbine Film Cooling”, Journal of Propulsion and Power, Vol. 22, n.° 2 , pp. 249-270.

[3] York, W. D. and Leylek, J. H., 2002, “Leading-Edge Film Cooling Physics: Part I- Adiabatic Effectiveness”, ASME paper GT-2002-30166

[4] Medic, G., and Durbin P. A., 2002, “Towards improved prediction of heat transfer in turbine blades”, Journal of Turbomachinery, Vol. 124, pp.187-192.

[5] Harrison, K. and Bogard, D. G., 2008, “Evaluation of the Use of the Adiabatic Wall Temperature to Predict Heat Fluxes for Film Cooled Turbine Airfoils”, ISROMAC 12-2008-20187.

[6] Keimasi, M.R., Taeibi-Rahni, M., 2001, “Numerical simulation of jets in a crossflow using different turbulence models”, AIAA Journal, Vol. 39, n. 12, pp. 2268-2277.

[7] FLUENT 6.3 User's Guide, 2006, Fluent Inc, Lebanon.

[8] Silieti, M., Divo, E., Kassab, A. J., 2004, "Numerical investigation of adiabatic and conjugate film cooling effectiveness on a single cylindrical film-cooling hole”, IMECE2004-62196.

[9] Silieti, M., Kassab, A. J., Divo, E., 2009, “Film cooling effectiveness: Comparison of adiabatic and conjugate heat transfer CFD models”, International Journal of Thermal Sciences, Vol. 48, n. 12, pp. 2237-2248.

[10] Na, S., Zhu, B., Bryden, M., Shih, T.I.-P., 2006, “CFD Analysis of film cooling”, 44th AIAA Aerospace Sciences Meeting, Vol. 1, pp. 292-301.

[11] Liu, C. L., Zhu, H. R., Bai, J. T., 2008, “Effect of turbulent Prandtl number on the computation of film-cooling effectiveness”, International Journal of Heat and Mass Transfer, Vol. 51, n. 25-26, pp. 6208-6218.

[12] Lee, K. D. and Kim, K. Y., Optimization of a cylindrical film cooling hole using surrogate modeling, 2009, Numerical Heat Transfer, Part A: Applications, Vol. 55, n. 4, pp. 362-380.

[13] Lee, K. D. and Kim, K. Y., 2010, Shape optimization of a fan-shaped hole to enhance film-cooling effectiveness, International Journal of Heat and Mass Transfer, Vol. 53, n. 15-16, pp. 2996-3005.

[14] Krishnababu, S.K., Hodson, H. P., Booth, G. D., Lock, G. D., Dawes, W. N., 2010, “Aerothermal investigation of tip leakage flow in a film cooled industrial turbine rotor”, Journal of Turbomachinery, Vol. 132, n. 2, pp. 1-9.

[15] Ledezma, G. A., Laskowski, G. M., Tolpadi, A. K., 2008, Turbulence model assessment for conjugate heat transfer in a high pressure turbine vane model”, ASME paper GT2008-50498.

[16] Lin, Y.-L and Shih, T.I-P., 2001, “Film Cooling of a Cylindrical Leading Edge with Injection Through Rows of Compound Angle Holes”, Journal of Heat Transfer , Vol.123, n. 4, pp. 645-654.

[17] Cruse, M. W., Yuki, U.M., Bogard, D.G., 1997, “Investigation of various parametric influences on leading edge film cooling”, ASME paper 97-GT-296.

[18] Thakur S., Wright J., Shyy W., 1999, “Convective film cooling over a representative turbine blade leading-edge”, International Journal of Heat and Mass Transfer, Vol. 42, pp. 2269-2285.

[19] Albert, J. E., Bogard, D. G., Cunha, F., 2004, “Adiabatic and overall effectiveness for a film cooled blade”, ASME paper GT2004-53998.

[20] Terrell, E. J, Mouzon, B. D., Bogard, D. G., 2005, “Convective Heat Transfer Through Film Cooling Holes of a Gas Turbine Blade Leading Edge”, ASME paper GT2005-69003.

[21] Dyson, T. E., Bogard, D. G., Piggush, J.D., Kohli, A., 2010, “Overall effectiveness for a film cooled turbine blade leading edge with varying hole pitch”, ASME paper GT2010-23707.

[22] Mills, A. F., 1999, Heat Transfer, Second edition, Prentice Hall, Inc.

[23] Ravelli, S., Dobrowolski, L., Bogard, D.G., 2010, “Evaluating the Effect of Internal Impingement Cooling on a Film Cooled Turbine Blade Leading Edge”, ASME Paper GT2010-23002.

[24] Polanka, M. D., Cutbirth, J. M., and Bogard, D. G., “Three Component Velocity Field Measurements in the Stagnation Region of a Film Cooled Turbine Vane,” *ASME Journal of Turbomachinery,* Vol. 124, pp. 445-452, 2002.